ELSEVIER

Physica A 249 (1998) 103–110

PHYSICA A

Formation of periodic and localized patterns in an oscillating granular layer

Igor S. Aranson [a,b,*,1], Lev S. Tsimring [c,2]

[a] *Bar Ilan University, Ramat Gan 52900, Israel*

[b] *Argonne National Laboratory, 9700 South Cass Avenue, Argonne, IL 60439, USA*

[c] *Institute for Nonlinear Science, University of California, San Diego, La Jolla, CA 92093-0402, USA*

Abstract

A simple phenomenological model for pattern formation in a vertically vibrated layer of granular particles is proposed. This model exhibits a variety of stable cellular patterns including standing rolls and squares as well as localized excitations (*oscillons* and *worms*), similar to recent experimental observations (Umbanhowar et al., 1996). The model is an order parameter equation for the parametrically excited waves coupled to the mass conservation law. The structure and dynamics of the solutions resemble closely the properties of patterns observed in the experiments. © 1998 Published by Elsevier Science B.V. All rights reserved.

The collective behavior of granular systems becomes one of the central issues of nonlinear dynamics. Transport, mixing, and segregation properties of large ensembles of granular particles are important for various industrial applications. Granular materials exhibit a unique mixture of properties of both liquids and solids. Intensive theoretical, numerical and experimental studies of granular systems revealed a wide variety of new phenomena, such as clustering and inelastic collapse, random-force chains and granular convection (see for review Ref. [1]). Various periodic and disordered patterns arise in vibrated granular layers [2–4]. The very complicated rheology of granular media makes their theoretical analysis extremely difficult. Unlike fluid dynamics, there is no reliable continuum description of a granular system applicable in a wide range of conditions. The widely used approach is a straightforward simulation of many inelastically interacting particles in a gravity field [5–7].

* Correspondence address: Bar Ilan University, Ramat Gan 52900, Israel.

[1] Supported by the U.S. DOE under contract W-31-109-ENG-38 and by NSF, Office of Science and Technology Center under contract DMR91-20000.

[2] Supported by the U.S. DOE under contract DE-FG03-96ER14592.

PII S0378-4371(97)00437-8

Vibrated granular systems often manifest fluid-like behavior which resembles similar phenomena in conventional liquids. Recent experimental studies of vertically vibrated granular systems [2–4] demonstrated a rich variety of collective behavior ranging from standing waves, hexagons, squares to localized excitations (particle-like *oscillons* [3] and quasi-one-dimensional *worms*, see Ref. [1]). Periodic patterns (squares, rolls and hexagons) are remarkably similar to well-known Faraday waves in fluids which have been a subject of intensive research (see, e.g. Refs. [8,9]). The important difference, however, is that the primary bifurcation to square patterns and oscillons is hysteretic. The localized objects, oscillating at half the frequency of plate vibrations $\Omega/2$ on the background of a flat surface oscillating at Ω, are observed in slightly subcritical parameter region. Although some features of collective behavior of vibrated granular systems were reproduced in simulations of a large ensemble of inelastically interacting particles [5–7], the macroscopic understanding of the dynamics is lacking. We propose a simple continuum model [10] exhibiting phenomenology remarkably similar to the experimental observations. The model is an order parameter equation for the parametrically excited medium coupled to the mass conservation law. Although this model is not derived from the corresponding microscopic equations of granular systems, it can be instructive for interpretation of experimental data and may yield testable predictions.

Phenomenological Equations. The model consists of an equation for the order parameter ψ coupled to a conservation law for the average mass of granular material per unit area (or a local averaged thickness of the layer):

$$\partial_t \psi = \gamma \psi^* - (1 - i\omega)\psi + (1 + ib)\nabla^2 \psi - |\psi|^2 \psi - \rho\psi \,, \tag{1}$$

$$\partial_t \rho = \alpha \nabla \cdot (\rho \nabla |\psi|^2) + \beta \nabla^2 \rho \,. \tag{2}$$

Eq. (1) without the last term is a popular model for the parametric instability in oscillating liquid layer (see Refs. [11,12]). We would like to emphasize that despite the absence of higher-order spatial derivatives, Eq. (1) is analogous to the Swift–Hohenberg equation rather than to the complex Ginzburg–Landau equation for slow long-wave amplitude. The order parameter $\psi(x, y, t)$ characterizes the complex amplitude of the particle oscillations ξ at the frequency of parametric resonance $\omega = \Omega/2$ according to $\xi(x, y, t) = \psi(x, y, t) \exp[i\Omega t/2] + \text{c.c}$ and, therefore, may exhibit fast spatial oscillations. Linear terms in Eq. (1) can be derived from the dispersion relation for parametrically driven granular waves, expanded near frequency ω and corresponding wave number k (here $k = \sqrt{\omega/b}$, parameter b must be chosen to reproduce the correct wave number at a given frequency). The term $\gamma\psi^*$ provides parametric driving and leads to the excitation of standing waves. The term $|\psi|^2\psi$ phenomenologically accounts for the nonlinear saturation of oscillations provided in granular materials by inelastic collisions. The last term in Eq. (1) accounts for the coupling of the order parameter to the local average density ρ. As it is observed experimentally [2–4], the threshold value of the vibration amplitude γ for the parametric instability depends on the mean layer thickness

[2,3] due to an increase of internal energy dissipation in thicker layers. Although one should generally expect this term to be $f(\rho)\psi$ with $f(\rho)$ saturating at large ρ (when the thickness of the layer is larger than the scale of typical perturbations), we hereafter limit ourselves with the simplest form $f(\rho)=\rho$ corresponding to relatively thin layers (proportionality constant can be omitted after appropriate scaling).

Eq. (2) describes the conservation of the granular material where ρ is a mass of granular material per unit square averaged over period of vibrations. Two different physical mechanisms contribute to the in-plane mass flux. The first term in Eq. (2) reflects the average particle drift due to the gradient of magnitude of high-frequency oscillations. On average, particles try to "escape" from regions of large fluctuations, the effect analogous to formation of so-called Chladni figures. The second term describes diffusive relaxation of the inhomogeneous mass distribution. We expect the effective "granular temperature" and corresponding diffusion constant β to be proportional to the energy of plate vibrations, then for nonvibrating plate the diffusion constant turns to zero and an arbitrary pattern "freezes".

Periodic patterns and their stability. Let us first consider the conditions for onset of oscillations in Eqs. (1) and (2). The trivial state $\psi=0$, $\rho=\rho_0$ corresponding to a flat layer oscillating at the plate vibration frequency Ω becomes unstable at $\gamma^2=\gamma_c^2=(\omega+b(1+\rho_0))^2/(1+b^2)$ for $\omega b>1+\rho_0$ with respect to a perturbation with the wave number k_c given by $k_c^2=(\omega b-1-\rho_0)/(1+b^2)$. For $\omega b<1+\rho_0$ spatially uniform perturbations with $k_c=0$ become unstable first and the vibration threshold is $\gamma_c^2=1+\rho+\omega^2$. Due to the rotational invariance of Eqs. (1) and (2), waves with all directions grow simultaneously. Above the threshold, the nonlinear terms in Eqs. (1) and (2) saturate the exponential growth of perturbations and provide pattern selection. In general, various patterns with different symmetries may coexist for the same parameters of the equations. For $\rho=$ const., Eqs. (1) and (2) reduce to a single equation for which it is known that rolls are the only stable cellular pattern above onset [11]. This has been a serious shortcoming of this model since square patterns are frequently observed in Faraday experiments [2,3,8]. It turns out that within our combined model with ρ being a dynamical variable squares and rolls emerge naturally in different parameter regions.

Let us now discuss the stability of simplest periodic patterns (rolls and squares) in the framework of Eqs. (1) and (2) close to the threshold of parametric instability. Within the framework of weakly nonlinear analysis (small supercriticality parameter ϵ is defined below), the periodic patterns are described by the following solution to Eq. (1): $\psi=(A\sin(k_c x)+B\sin(k_c y))\,e^{i\phi}+O(\epsilon)$, where $A(t)$, $B(t)$ are the real amplitudes of two (orthogonal) standing waves, $\phi=$ const. is given by solution of linearized problem. At the threshold ρ is enslaved to $|\psi|^2$ (this approximation is valid for $\alpha,\beta\gg\epsilon$), and follows the quasi-stationary solution of Eq. (2) $\rho=\rho_0(t)\exp[-\eta|\psi|^2]$, where $\eta=\alpha/\beta$. The function $\rho_0(t)$ can be found from the condition of total-mass conservation $S^{-1}\int\rho\,dx\,dy=\mu=$ const., S is the total area. Thus, we obtain the following expression (keeping for simplicity only the terms of the order of $\eta^2|\psi|^4$) in

the expansion of the exponent

$$\rho_0 = \frac{16\mu}{3\eta^2(A^4 + 4A^2B^2 + B^4) - 8\eta(A^2 + B^2) + 16}. \tag{3}$$

Substituting ρ into Eq. (1) and performing standard orthogonalization procedure to keep w small, we obtain the following equations for $A(t)$, $B(t)$ (we retain only two first orders of nonlinearity)

$$\dot{A} = A\left[\epsilon + \frac{\mu\eta - 3}{4}A^2 + \frac{2\mu\eta - 3}{2}B^2 - \frac{\mu\eta^2}{2}(B^2A^2 + 2B^4)\right]. \tag{4}$$

Equation for $B(t)$ is obtained by the permutation $A \Leftrightarrow B$. The supercriticality parameter is given by $\epsilon = \gamma_c(\gamma - \gamma_c)/(1 + \mu + k_c^2)$ [13]. It follows from Eq. (4) that hysteretic transition to squares ($A = B$) occurs if $\mu\eta > \frac{9}{5}$ and rolls ($A \neq 0$, $B = 0$ or $A = 0$, $B \neq 0$) exhibit subcritical bifurcation at $\mu\eta > 3$.

In the supercritical case we can drop the last term in Eq. (4). It is easy to verify that for $\epsilon \to +0$ the square pattern ($A = B$) is stable for $\mu\eta > 1$ and unstable otherwise. Rolls, in the limit $\epsilon \to +0$, are stable for $\mu\eta < 1$ and unstable otherwise. For larger $\epsilon > 0$ the higher-order terms in Eq. (4) become important, and squares are stable at $16\mu\epsilon\eta^2 < 3(10\epsilon\eta - \epsilon^2\eta^2 - 9)$ and rolls are stable at $4\mu\epsilon\eta^2 > 3(\epsilon\eta - \epsilon^2\eta^2 - 3)$. In the subcritical case $\eta\mu > \frac{9}{5}$ squares are stable in their entire basin of existence given by the condition $48\mu\epsilon\eta^2 + (5\eta\mu - 9)^2 = 0$. The phase diagram for roll and squares is shown in Fig. 1. It is qualitatively consistent with the experimental observations of transition from rolls to squares with decreasing the driving frequency if one assumes that $\eta\mu$ decreases with increase of frequency. One expects that the relative effect of particle drift from regions of intense fluctuations characterized by parameter η diminishes with the increase of ω since characteristic vertical scale of the layer involved in oscillations

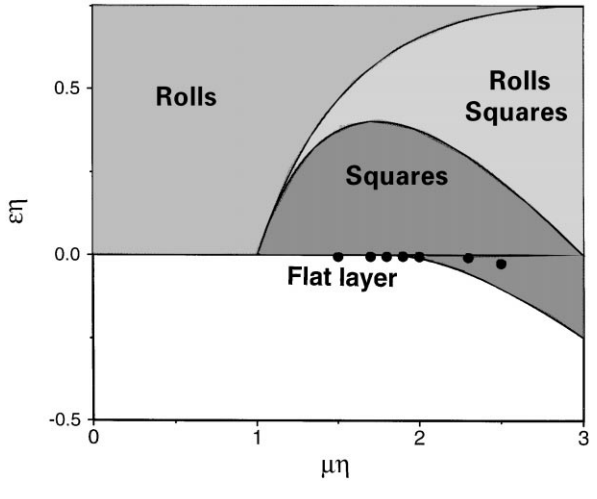

Fig. 1. Phase diagram for square and roll patterns, weakly nonlinear theory. Black dots indicate stable oscillons seen in numerical experiments.

becomes smaller at high frequencies. Also in agreement with experiments [2,3], there is a bistable region where rolls and squares co-exist. It should be noted however, that the phase diagram of Eq. (4) exactly corresponds to the original model given by Eqs. (1) and (2) only in the limit of small amplitude, otherwise it represents only a Galerkin approximation of the exact solution. Still, our simulations agreed fairly well with these stability limits.

Localized solutions. In experiments [4] oscillons appear slightly below the threshold of the parametric instability for cellular patterns. We also observed stationary localized axisymmetric solutions to Eqs. (1) and (2) in weakly subcritical region (dots in Fig. 1 correspond to stable localized solutions found for various combinations of parameters). In order to find a detailed structure of the localized solution, we solved stationary radially symmetric Eqs. (1) and (2) using matching–shooting method with Newton iterations. Fig. 2 shows the radial structure of the order parameter ψ and corresponding distribution of ρ for such solution. This solution corresponds to a dip in the average-mass distribution $\rho = \rho_0 \exp(-\eta|\psi|^2)$. Due to the symmetry $\psi \to -\psi$, oscillons of opposite polarities may coexist in this system. As it follows from Fig. 2, the solution has oscillating tails at $r \gg 1$, $\psi(r) \propto r^{-1/2}\exp(pr)$ with the (complex) exponent p given by $p^2 = -k_c^2 + \sqrt{(\gamma^2 - \gamma_c^2)/(1+b^2)}$. Since ψ is an amplitude of oscillations at half the driving frequency, peaks and craters with elevated periphery replace each other on consecutive cycles of plate vibrations. We studied the linear stability of these localized solutions with respect to axisymmetric (usually the most dangerous) perturbations. We found that the stability region is limited both at large and small γ in accord with experiments: $\gamma_{c1} < \gamma < \gamma_{c2} < \gamma_c$. At the edges of the stable region, $\gamma_{c1,2}$, stable solution corresponding to the oscillon annihilates with other unstable localized solutions.

The interaction of two oscillons can be considered in the spirit of Ref. [14]. It is natural to expect a variety of bound states, since the asymptotic behavior of ψ for the oscillon is oscillatory. A numerically found bound states of two oscillons with opposite phases is shown in Fig. 3b, and a bound state of four oscillons (one positive surrounded by three negative) is shown in Fig. 3c. As in the experiment [3] we found that bound states with coordination numbers higher than three are unstable. There also exists a stable bound state of two like-phased oscillons (Fig. 3a), but the equilibrium distance between the oscillons is substantially larger than for oppositely phased pairs, resulting in much weaker binding. Small "granular noise" probably unbinds such weakly coupled pairs.

We studied the nonlinear evolution of oscillons beyond their region of stability in numerical simulations of Eqs. (1) and (2). Once the lower bound γ_{c1} is passed, the oscillon rapidly decays towards a trivial state $\psi = 0$. After increasing γ above γ_{c2} initial spreading leads to a range of different scenarios depending on other parameters $\eta, \mu, \omega, \alpha$. For small $\eta\mu$ (supercritical transition) oscillons produce a sequence of concentric rolls. Depending on $\eta\mu$ they either remain rolls or break to produce a disordered square pattern. At larger $\eta\mu$ oscillon produces other oscillons on its periphery as

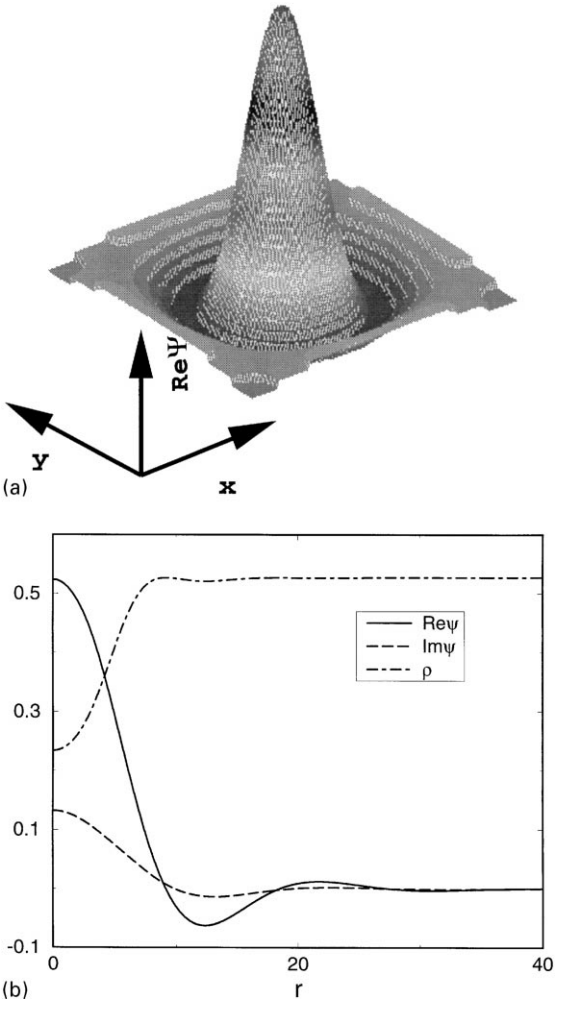

Fig. 2. (a) 3D plot of $\mathrm{Re}\,\psi$ and (b) radial structure of the stable oscillon for $\gamma = 1.8, \mu = 0.527, b = 2$, $\omega = \alpha = 1$, $\eta = 2.78$.

seen in experiments [4]. It turns out, surprisingly, that following oscillons do not appear uniformly around the center but rather organize themselves in chains, resembling worm-like patterns (Fig. 3d–Fig. 3f), cf. photo by Umbanhowar published in Ref. [1]. We propose explanation of this effect by the conservation of total mass. Oscillons push the granular material on their periphery. Since the excessive mass from oscillons in a chain is redistributed by the diffusion, it spreads more rapidly near the tip of the chain. Therefore, the next oscillon will likely appear there, and the tip advances. This process will continue until the average density in the surrounding flat regions becomes so high that the creation of new oscillons is halted (the threshold for oscillon stability γ_{c2}

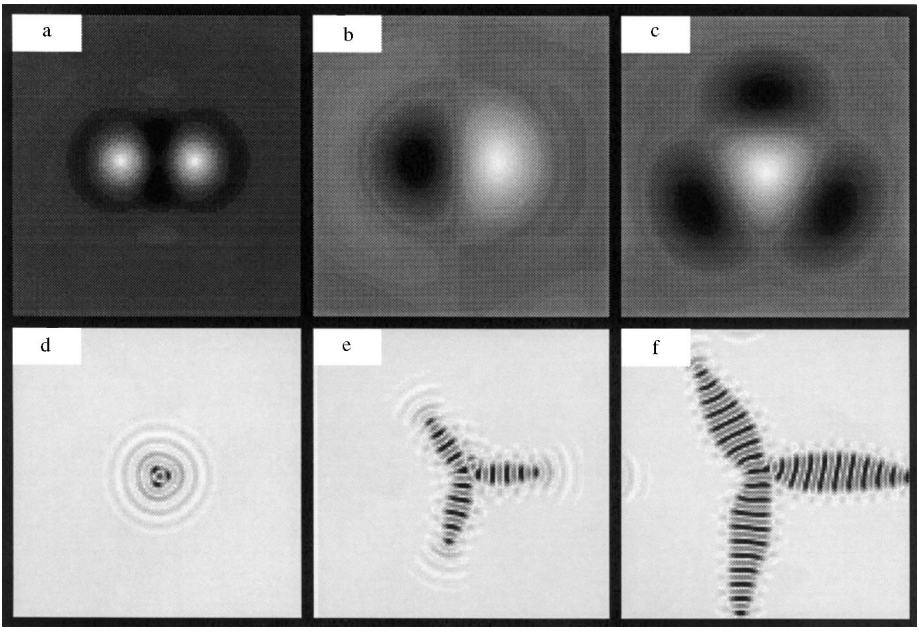

Fig. 3. Gray-coded images of $\mathrm{Re}\,\psi$ (black corresponds to maximum, white to minimum) from simulations of Eqs. (1) and (2). Bound states of oscillons for $\alpha = \omega = 1$, $b = 2$, $\eta = 2.78$, $\mu = 0.527$, $\gamma = 1.8$: (a) likely phased oscillons, size $L = 100$; (b) oppositely phased oscillons, $L = 40$; (c) triangular bound state, same parameters; (d–f) worm-like structure produced by a single oscillon in the center, $\alpha = 1$, $\omega = b = 2$, $\gamma = 2.245$, $\eta = 4.38$, $\mu = 0.525$, $L = 100$.

increases with the average density). Our simulations show that for values of γ slightly above γ_{c2} even after a long time, oscillons do not fill entire area (see Fig. 3f).

We have shown on the basis of phenomenological model that the constraint of mass conservation plays a crucial role in pattern formation in vibrated granular materials. We can speculate that our results may also be relevant for fluids, where square patterns are ubiquitous and confined states were also observed recently [15]. Since parametric waves on a fluid surface induce mean surface displacement obeying a conservation law, we believe that a coupled set of equations for the order parameter and a mean displacement may serve as a paradigm model for this system. We can also speculate that our model with minor modification is capable to describe more complicated spiral patterns observed in experiments with granular layers.

We thank M.I. Rabinovich, M. Mungan, H.L. Swinney, P. Umbanhowar, H. Levine, E. Brenner, and J. Fineberg for fruitful discussions.

References

[1] H.M. Jaeger, S.R. Nagel, R.P. Behringer, Rev. Mod. Phys. 68 (1996).
[2] F. Melo, P. Umbanhowar, H.L. Swinney, Phys. Rev. Lett. 72 (1994) 172.
[3] F. Melo, P. Umbanhowar, H.L. Swinney, Phys. Rev. Lett. 75 (1995) 3838.
[4] P. Umbanhowar, F. Melo, H.L. Swinney, Nature 382 (1996) 793.
[5] G.H. Ristow, H.J. Herrmann, Phys. Rev. E 50 (1994) R5.
[6] S. Luding et al., Europhys. Lett. 36 (1996) 247.
[7] K.M. Aoki, T. Akiyama, Phys. Rev. Lett. 77 (1996) 4166.
[8] See, e.g., A.B. Ezersky et al., Sov. Phys. – JETP 64 (1986) 1228.
[9] N.B. Tufillaro, R. Ramshankar, J.P. Gollub, Phys. Rev. Lett. 62 (1989) 422.
[10] L.S. Tsimring, I. Aranson, Phys. Rev. Lett. 79 (1997) 213.
[11] W. Zhang, J. Vinals, Phys. Rev. Lett. 74 (1995) 690.
[12] S.V. Kiyashko et al., Phys. Rev. E 54 (1996) 5037.
[13] The terms $O(A^5, B^5)$ in Eq. (4) coming from the coupling of the primary waves with their higher harmonics are small for high internal friction ($\mu \ll 1$, $\eta \gg 1$).
[14] I.S. Aranson et al., Physica D 43 (1990) 436.
[15] O. Lioubashevsky, H. Arbell, J. Fineberg, Phys. Rev. Lett. 76 (1996) 3959.